Silicon Photonics
矽光子學
4 Silicon-On-Insulator (SOI) Photonics (C)

課程編號：941 U0460
科目名稱：矽光子學
授課教師：黃鼎偉
時間地點：一678 明達館 303

Outline

- 4.7 COUPLING TO THE OPTICAL CIRCUIT
- 4.8 OPTICAL MODULATION MECHANISMS IN SILICON
- 4.9 OTHER ADVANTAGES AND DISADV ANT AGES OF SILICON PHOTONICS

4.7 COUPLING TO THE OPTICAL CIRCUIT

COUPLING TO THE OPTICAL CIRCUIT

- Butt coupling
  - directly overlap the waveguide ends
- End-fire coupling
  - focus the beam through a lens
- Prism coupling
  - Surface coupling at a specific angle for each waveguide mode
  - Prism should have a higher refractive index than the core
- Grating coupling
  - Surface coupling through diffraction

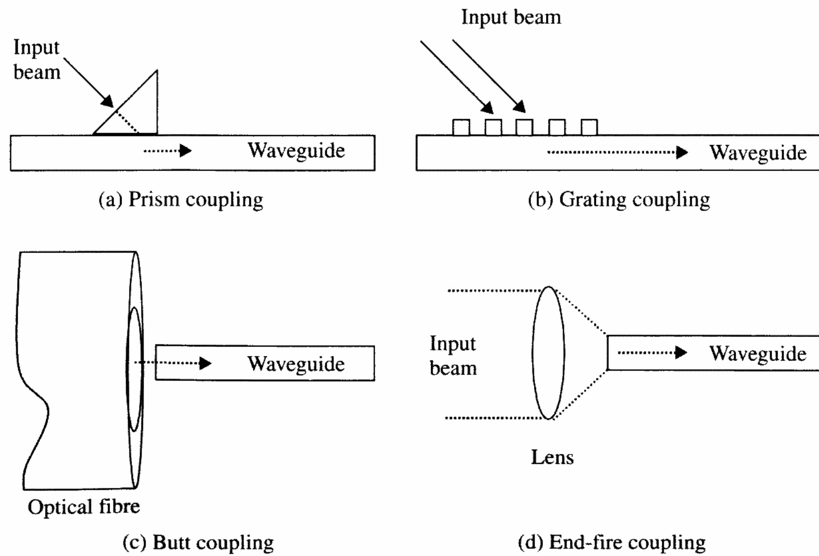

Figure 4.11 Four techniques for coupling light to optical waveguides

4.7.1 Grating Couplers

Grating Couplers

- Phase matching condition
  - the components of the phase velocities in the direction of propagation (*z* direction) to be the same.

$$k_z = k_0 n_3 \sin\theta_a \qquad \beta = k_z = k_0 n_3 \sin\theta_a$$

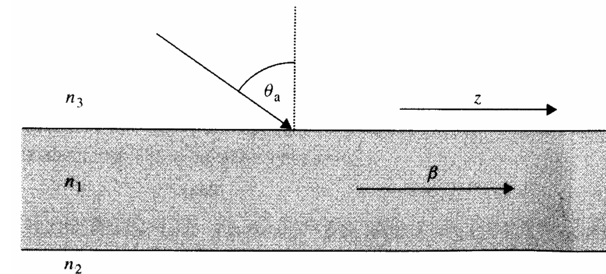

Figure 4.12 Light incident upon the surface of a waveguide

Grating Couplers

- Grating can be used as input and out coupler
  - Propagation constant of the waveguide (without grating) β_W
  - Possible propagation constant due to the index modulation of the grating β_p

$$\beta_p = \beta_W + \frac{2p\pi}{\Lambda}$$

  - Λ is the grating period, $p = \pm 1, \pm 2, \pm 3, \ldots$
  - But only negative value of *p* can be used for coupling into the waveguide, usually *p* = -1.

$$\beta_p = \beta_W - \frac{2\pi}{\Lambda}$$

Grating Couplers

- Thus,

$$\beta_W - \frac{2\pi}{\Lambda} = k_0 n_3 \sin\theta_a$$

  - *N*: the effective index of the waveguide mode

$$k_0 N - \frac{2\pi}{\Lambda} = k_0 n_3 \sin\theta_a$$

$$\Lambda = \frac{\lambda}{N - n_3 \sin\theta_a}$$

  - n_3 is usually 1 (air).

$$\Lambda = \frac{\lambda}{N - \sin\theta_a}$$

Grating Couplers

- Because the refractive index of silicon is large, the required period of grat-ings in silicon for input/output coupling is of the order of 400 nm.
- The highest coupling efficiencies from gratings in silicon have been reported
  - an output coupling efficiency of approximately 70 % for rectangular gratings.
  - 84 % for gratings with a nonsymmetrical profile.
- A deep etch perturbs the refractive index of a given waveguide more than does a shallow grating, hence enabling the coupling mechanism, it may also add more loss due to increased scattering because of the increased abruptness of the refractive index.

Grating Couplers

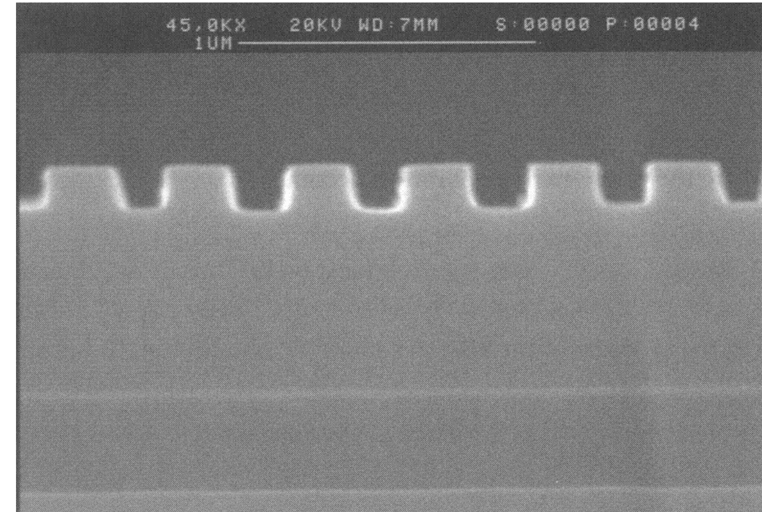

Figure 4.13 Waveguide coupler fabricated in the silicon layer of an SOI waveguide.

4.7.2 Butt Coupling and End-fire Coupling

Butt Coupling and End-fire Coupling

- The coupling efficiency is a function of
  - (i) how well the fields of the excitation and the waveguide modes match;
  - (ii) the degree of reflection from the waveguide facet;
  - (iii) the quality of the waveguide endface;
  - (iv) the spatial misalignment of the excitation and waveguide fields.
  - (v) the numerical aperture mismatch in which the input angles of the optical waveguide are not well matched to the range of excitation angles
  - (vi) the match of polarization

(i) Overlap of Excitation and Waveguide Fields

- Overlap integral: Γ

$$\Gamma = \frac{\int_{-\infty}^{\infty} \mathrm{d}y \int_{-\infty}^{\infty} E\varepsilon \mathrm{d}x}{\left[\int_{-\infty}^{\infty} \mathrm{d}y \int_{-\infty}^{\infty} E^2 \mathrm{d}x \cdot \int_{-\infty}^{\infty} \mathrm{d}y \int_{-\infty}^{\infty} \varepsilon^2 \mathrm{d}x\right]^{\frac{1}{2}}}$$

  - *E*: the waveguide field
  - ε : the excitation field
  - The factor Γ lies between 0 and 1.

(i) Overlap of Excitation and Waveguide Fields

- By Gaussian approximation of the fields

$$E = \exp\left[-\left(\frac{x^2}{\omega_x^2} + \frac{y^2}{\omega_y^2}\right)\right] \qquad \varepsilon = \exp\left[-\frac{(x^2+y^2)}{\omega_0^2}\right]$$

  - Using the mathematical identity

$$\int_0^{\infty} \exp[-r^2x^2]\,\mathrm{d}x = \frac{\sqrt{\pi}}{2r}$$

  - Thus, field coupling efficiency

$$\Gamma = \frac{\frac{2}{\omega_0}\left[\frac{1}{\omega_x\omega_y}\right]^{\frac{1}{2}}}{\left[\frac{1}{\omega_x^2} + \frac{1}{\omega_0^2}\right]^{\frac{1}{2}}\left[\frac{1}{\omega_y^2} + \frac{1}{\omega_0^2}\right]^{\frac{1}{2}}}$$

(i) Overlap of Excitation and Waveguide Fields

- Power Coupling Efficient

$$\Gamma^2 = \frac{\frac{4}{\omega_0^2}\left[\frac{1}{\omega_x\omega_y}\right]}{\left[\frac{1}{\omega_x^2} + \frac{1}{\omega_0^2}\right]\left[\frac{1}{\omega_y^2} + \frac{1}{\omega_0^2}\right]}$$

Table 4.2

ω_0	ω_x	ω_y	Γ	Γ^2	Loss due to Γ^2 (dB)
5 µm	5 µm	5 µm	1.0	1.0	0
10 µm	10 µm	5 µm	0.894	0.8	0.97
20 µm	16 µm	3 µm	0.535	0.286	5.4
20 µm	1 µm	1 µm	0.1	0.01	20
5 µm	5 µm	3 µm	0.939	0.882	0.55
5 µm	4.8 µm	4.9 µm	0.999	0.999	0.004

(ii) Reflection from the Waveguide Facet

- Reflection coefficient for TE polarization

$$r_{TE} = \frac{n_1 \cos\theta_1 - n_2 \cos\theta_2}{n_1 \cos\theta_1 + n_2 \cos\theta_2} \qquad r_{TE} = \frac{-\sin(\theta_1 - \theta_2)}{\sin(\theta_1 + \theta_2)}$$

- Reflection coefficient for TM polarization

$$r_{TM} = \frac{n_2 \cos\theta_1 - n_1 \cos\theta_2}{n_2 \cos\theta_1 + n_1 \cos\theta_2}$$

- Reflectivity $R = |r|^2$

$$R_{TE} = r_{TE}^2 = \frac{\sin^2(\theta_1 - \theta_2)}{\sin^2(\theta_1 + \theta_2)} \qquad R_{TM} = r_{TM}^2 = \frac{\tan^2(\theta_1 - \theta_2)}{\tan^2(\theta_1 + \theta_2)}$$

(ii) Reflection from the Waveguide Facet

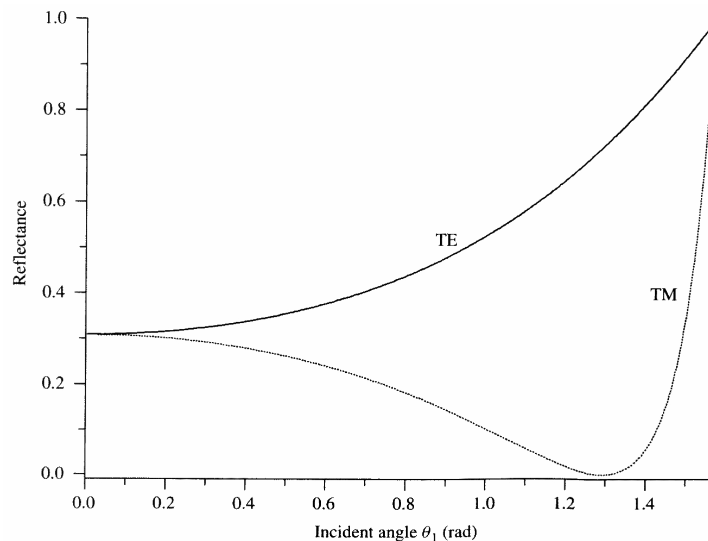

Figure 4.14 Reflection at an air/silicon interface

(ii) Reflection from the Waveguide Facet

- Normal incident
  - 31% (1.6 dB loss)

$$R = \left| \frac{n_1 - n_2}{n_1 + n_2} \right|^2$$

- Single-layer Anti-reflection Coating (V-coating)

$$R = \left| \frac{n_1 n_2 - n_{ar}^2}{n_1 n_2 + n_{ar}^2} \right|^2$$

  - Refractive Index

$$n_1 n_2 = n_{ar}^2$$

  - Thickness: $t_{ar} = \lambda/4 = \lambda_0/4n_{ar}$
  - Can be achieved by using Silicon Oxynitride SiO_xN_y (SiO_2 1.46 – Si_3N_4 2.05)

(iii) ***The Quality of the Waveguide Endface***

- Cleaving
  - The quality is excellent for crystalline silicon wafer
  - Varies for SOI wafer
- Polishing
  - Most common method
  - Polish by lapping with abrasives with sequentially decreasing grit sizes
- Etching
  - Chemical or Dry etching

(iv) **Spatial Misalignment of the Excitation and Waveguide Fields**

- For the Waveguide and Excitation Fields

$$E = \exp\left[-\left(\frac{x^2}{\omega_x^2} + \frac{y^2}{\omega_y^2}\right)\right] \quad \varepsilon = \exp\left[-\frac{(x^2+y^2)}{\omega_0^2}\right]$$

- The coupling efficiency is

$$\Gamma = \frac{\int_{-\infty}^{\infty} \mathrm{d}y \int_{-\infty}^{\infty} E\varepsilon \mathrm{d}x}{\left[\int_{-\infty}^{\infty} \mathrm{d}y \int_{-\infty}^{\infty} E^2 \mathrm{d}x \cdot \int_{-\infty}^{\infty} \mathrm{d}y \int_{-\infty}^{\infty} \varepsilon^2 \mathrm{d}x\right]^{\frac{1}{2}}}$$

(iv) **Spatial Misalignment of the Excitation and Waveguide Fields**

- The coupling efficiency is decreased by a factor

$$\psi = \exp\left[-\frac{A^2}{\omega_y^2 + \omega_0^2}\right]$$

- For $w_y = w_0 = 5\ \mu\mathrm{m}$,
- $A = 2\ \mu\mathrm{m}$
  - $\psi = 0.85$ (0.7 dB)

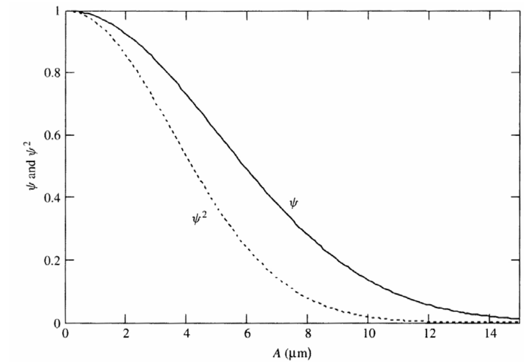

Figure 4.15 Effect of an offset *A* on the electric field overlap and the power coupling efficiency

(iv) **Spatial Misalignment of the Excitation and Waveguide Fields**

- If the Excitation Field is mis-aligned with an offset A in the y direction

$$\varepsilon = \exp\left[-\frac{(x^2+(y-A)^2)}{\omega_0^2}\right] \quad \text{or} \quad \varepsilon = \exp\left[-\frac{(x^2+(y^2+A^2-2Ay))}{\omega_0^2}\right]$$

- The coupling efficiency is then

$$\Gamma^{\mathrm{I}} = \exp\left[-\frac{A^2}{\omega_y^2+\omega_0^2}\right] \cdot \frac{\int_{-\infty}^{\infty} \mathrm{d}y \int_{-\infty}^{\infty} E\varepsilon \mathrm{d}x}{\left[\int_{-\infty}^{\infty} \mathrm{d}y \int_{-\infty}^{\infty} E^2 \mathrm{d}x \cdot \int_{-\infty}^{\infty} \mathrm{d}y \int_{-\infty}^{\infty} \varepsilon^2 \mathrm{d}x\right]^{\frac{1}{2}}}$$

$$= \exp\left[-\frac{A^2}{\omega_y^2+\omega_0^2}\right]\Gamma$$

Robust Coupling to Waveguides for Commercial Applications

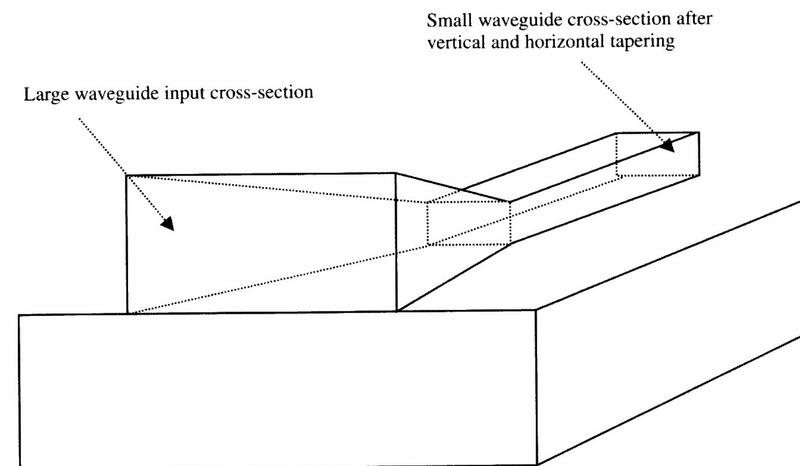

Figure 4.16 Schematic of vertical and horizontal waveguide tapers

Robust Coupling to Waveguides for Commercial Applications

- Insertion loss of less than 0.5 dB/facet

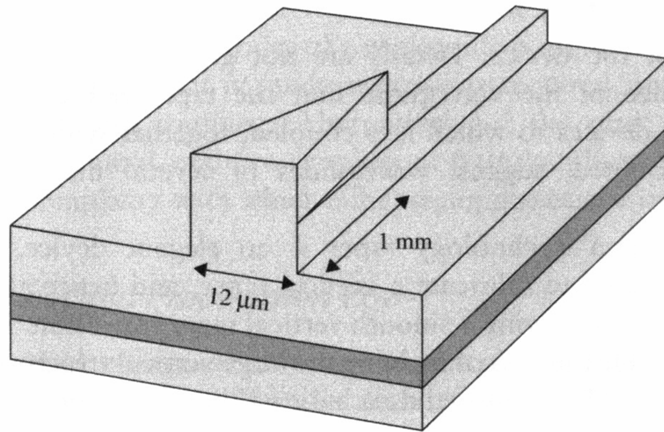

Figure 4.17 NVT taper to aid waveguide coupling, from Bookham Technology.

Robust Coupling to Waveguides for Commercial Applications

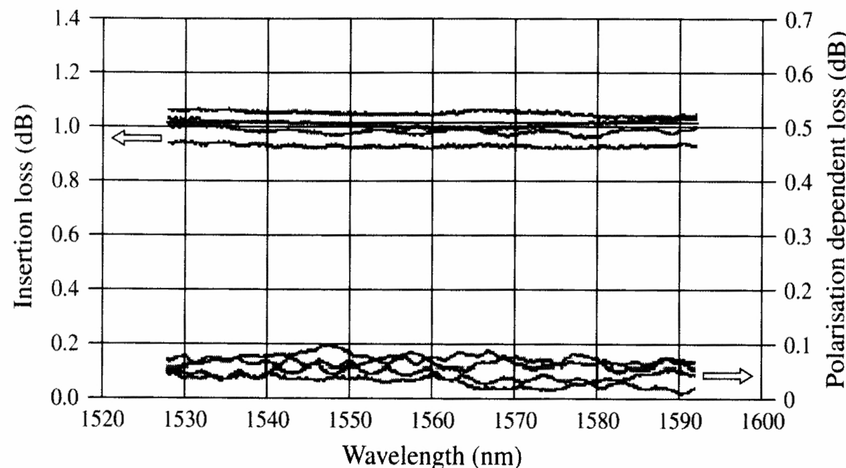

Figure 4.18 Fiber-to-fiber performance of two of Bookham Technology's NVT taper, connecting the two fibers to a variable optical attenuator.

Measurement of Propagation Loss in Integrated Optical Waveguides

- Loss for particular modes of a waveguide
  - mode selective approaches such as prism coupling or grating coupling can be used
- Total loss of the waveguide
  - end-fire coupling or butt coupling are attractive owing to the simplicity

Insertion Loss and Propagation Loss

- *Insertion Loss*
  - The insertion loss of a waveguide or device is the total loss associated with introducing that element into a system
  - Include both the inherent loss of the waveguide itself and the coupling losses associated with exciting the device.
- *Propagation Loss*
  - Loss associated with propagation in the waveguide or device, excluding coupling losses.

Loss Measurement Methods

- (i) the cut-back method
- (ii) the Fabry-Perot resonance method
- (iii) scattered light measurement

(i) The Cut-Back Method

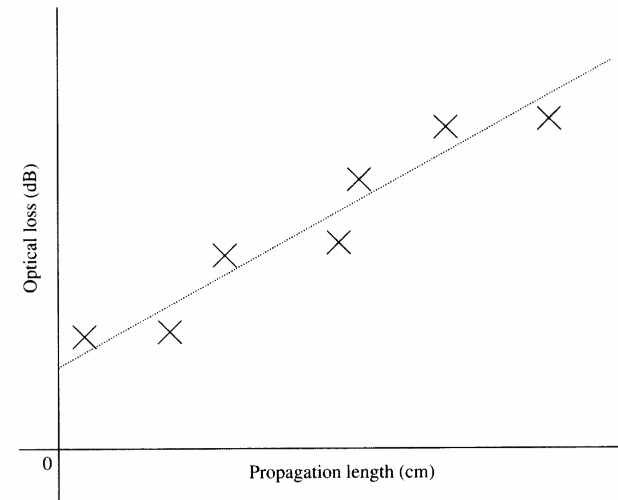

Figure 4.19 Scatter of optical loss measurements with waveguide length

(i) The Cut-Back Method

- A waveguide of length L_1
  - then cut short to become L_2

$$\frac{I_1}{I_2} = \exp[-\alpha(L_1 - L_2)]$$

The propagation loss

$$\alpha = \left(\frac{1}{L_1 - L_2}\right)\ln(I_2/I_1)$$

(ii) *The Fabry-Perot Resonance Method*

- *Fabry-Perot cavity formed by the endfaces.*
- *Transmittance*

$$\frac{I_t}{I_0} = \frac{(1-R)^2 e^{-\alpha L}}{(1-Re^{-\alpha L})^2 + 4Re^{-\alpha L}\sin^2(\phi/2)}$$

- *Maximum and Minimum Transmittances*

$$\frac{I_{max}}{I_0} = \frac{(1-R)^2 e^{-\alpha L}}{(1-Re^{-\alpha L})^2}$$

$$\frac{I_{min}}{I_0} = \frac{(1-R)^2 e^{-\alpha L}}{(1-Re^{-\alpha L})^2 + 4Re^{-\alpha L}} = \frac{(1-R)^2 e^{-\alpha L}}{(1+Re^{-\alpha L})^2}$$

(ii) ***The Fabry-Perot Resonance Method***

- Ratio of the maximum to the minimum

$$\zeta = \frac{I_{\max}}{I_{\min}} = \frac{(1 + Re^{-\alpha L})^2}{(1 - Re^{-\alpha L})^2}$$

- Thus, the propagation loss

$$\alpha = -\frac{1}{L} \ln\left(\frac{1}{R}\frac{\sqrt{\zeta} - 1}{\sqrt{\zeta} + 1}\right)$$

(ii) ***The Fabry-Perot Resonance Method***

- αL = 0.023

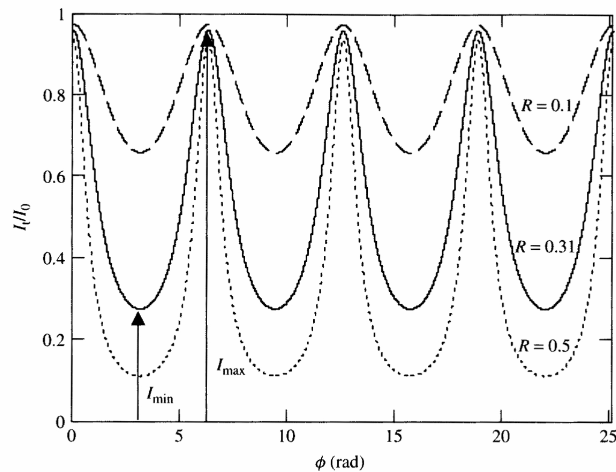

Figure 4.20 Plot of the Fabry-Perot transfer function for three different mirror reflectivities

(ii) ***The Fabry-Perot Resonance Method***

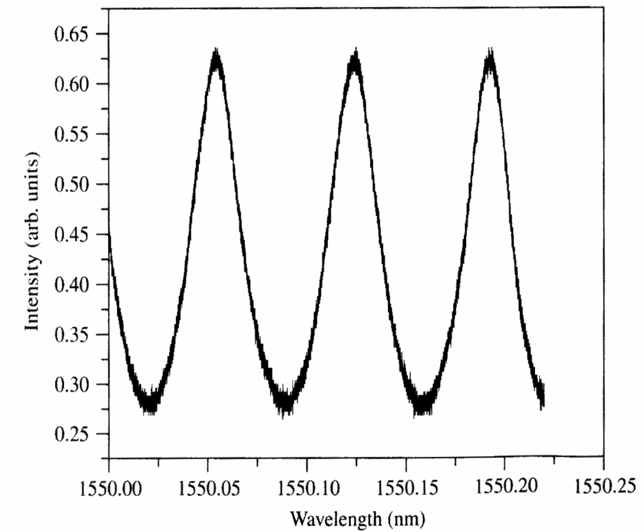

Figure 4.21 Fabry-Perot scan of a single-mode waveguide.

(ii) ***The Fabry-Perot Resonance Method***

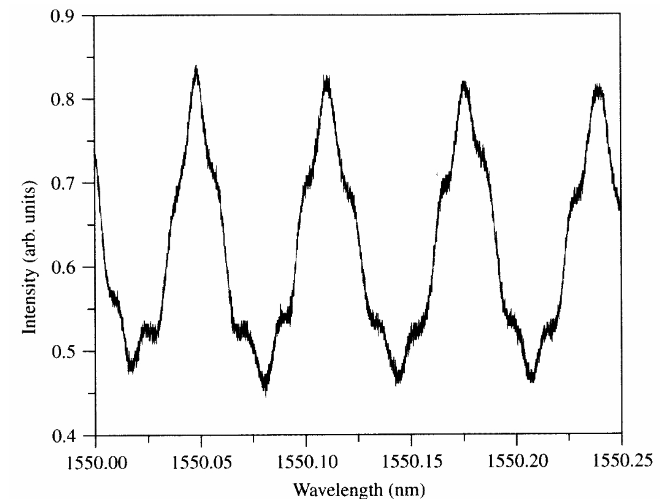

Figure 4.22 Fabry-Perot scan of a multi mode waveguide.

(iii) Scattered Light Measurement

- The measurement of scattered light from the surface of a waveguide can be used to determine the loss.
- Optical fibers can be used to collect scattered light from the surface of a waveguide, and can be scanned along the surface
- An image of the entire surface can be made, and the decay of scattered light determined accordingly.
  - Only suitable for the waveguide with high propagation loss due to scattering.

4.8 OPTICAL MODULATION MECHANISMS IN SILICON

(i) Electric Field Effects

- *Electrorefraction*: a change in real refractive index, Δn, with an applied electric field (also known as EO)
- *Electroabsorption:* a change in the imaginary part of refractive index, $\Delta \alpha$, with applied electric field (also known as EA)

(i) Electric Field Effects

- ***The Pockels Effect*** (also known as the linear electro-optic effect)
  - The real refractive index change, Δn, which is proportional to the applied field, E

$$\Delta n = -r_{33} n_{33} \frac{E_3}{2}$$

  - It is dependent upon the direction of the applied electric field with respect to the crystal axes.
  - For lithium niobate ($LiNbO_3$)
    ⇨ $r_{33} = 30.8 \times 10^{-12}$ m/V
  - Silicon has no Pockels Effect due to centro-symmetric crystalline structure

(i) Electric Field Effects

- ***The Kerr Effect*** (also known as the second order (nonlinear) electro-optic effect)
  - The real refractive index change, Δn, which is proportional to the square of the applied field, E

$$\Delta n = s_{33} n_0 \frac{E^2}{2}$$

  - It is dependent upon the direction of the applied electric field with respect to the crystal axes.
  - For Silicon, $s_{33} \cong 10^{-20}$ $(V/m)^2$

(i) Electric Field Effects

- ***The Franz-Keldysh Effect***
  - Both electrorefraction and electro absorption (major) near the Band Edge (1.07 μm) due to distortion of the energy bands of the semiconductor upon application of an electric field.
  - The effect diminishes significantly at the telecommunications wavelengths of 1.31 μm and 1.55 μm.
  - For Silicon, at 1.07 μm, if E = 2×10^5 V/cm ⇨ $\Delta n = 10^{-4}$

(i) Electric Field Effects

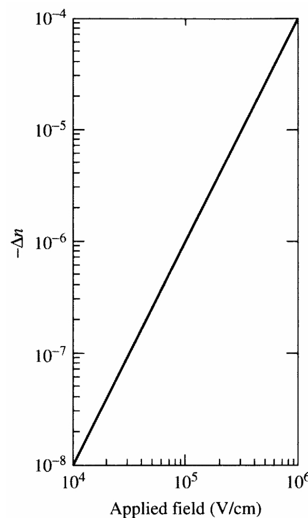

Figure 4.23 The Kerr effect in silicon as a function of applied electric field, at 300 K and A = 1.3 μm.

(i) Electric Field Effects

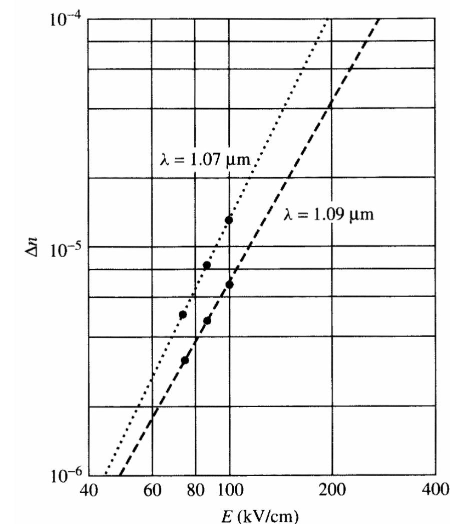

Figure 4.24 The Franz- Keldysh effect in silicon at 300 K and for two values of λ

(ii) Carrier Injection or Depletion

- Drude-Lorentz Equation
  - For absorption

$$\Delta\alpha = \frac{e^3\lambda_0^2}{4\pi^2c^3\varepsilon_0 n}\left(\frac{N_e}{\mu_e(m^*_{ce})^2} + \frac{N_h}{\mu_h(m^*_{ch})^2}\right)$$

  - For refractive index

$$\Delta n = \frac{-e^2\lambda_0^2}{8\pi^2c^2\varepsilon_0 n}\left(\frac{N_e}{m^*_{ce}} + \frac{N_h}{m^*_{ch}}\right)$$

(ii) Carrier Injection or Depletion

- In silicon

At $\lambda_0 = 1.55\ \mu m$:

$$\Delta n = \Delta n_e + \Delta n_h = -[8.8 \times 10^{-22}\Delta N_e + 8.5 \times 10^{-18}(\Delta N_h)^{0.8}]$$
$$\Delta\alpha = \Delta\alpha_e + \Delta\alpha_h = 8.5 \times 10^{-18}\Delta N_e + 6.0 \times 10^{-18}\Delta N_h$$

At $\lambda_0 = 1.3\ \mu m$:

$$\Delta n = \Delta n_e + \Delta n_h = -[6.2 \times 10^{-22}\Delta N_e + 6.0 \times 10^{-18}(\Delta N_h)^{0.8}]$$
$$\Delta\alpha = \Delta\alpha_e + \Delta\alpha_h = 6.0 \times 10^{-18}\Delta N_e + 4.0 \times 10^{-18}\Delta N_h$$

- For example, $\Delta N = 5\times10^{17}$

$$\Delta n = -[6.2 \times 10^{-22}(5 \times 10^{17}) + 6.0 \times 10^{-18}(5 \times 10^{17})^{0.8}]$$
$$= -1.17 \times 10^{-3}$$

(iii) The Thermo-optic Effect

- The thermo-optic coefficient in silicon

$$\frac{dn}{dT} = 1.86 \times 10^{-4}/\text{K}$$

  - 6ºC temperature variation
    - ⇨ Refractive index change $\Delta n = +1.1\times10^{-3}$
  - For a 500 μm silicon waveguide device for the π phase change
    - ⇨ Required power = 10 mW, 7ºC variation and $\Delta n = +1.3\times10^{-3}$

4.9 OTHER ADVANTAGES AND DISADV ANT AGES OF SILICON PHOTONICS

Table 4.3

Advantages of silicon photonics	Disadvantages of silicon photonics
i. Stable, well-understood material	i. No Pockels effect
ii. Stable native oxide available for cladding/electrical isolation	ii. indirect bandgap means native optical sources are not possible
iii. Relatively low-cost substrates	iii. High refractive index means inherently short devices are difficult to fabricate (e.g. gratings)
iv. Optically transparent at important wavelengths of 1.3 μm and 1.55 μm	iv. Modulation mechanisms tend to be relatively slow
v. Well-characterised processing	v. Thermal effects can be problematic for some optical circuits
vi. Highly confining optical technology	
vii. High refractive index means short devices	
viii. Micromachining means V-grooves and an effective hybrid technology are possible	
ix. Semiconductor material offers the potential of optical and electronic integration	
x. High thermal conductivity means high-power devices or high packing density may be tolerated	
xi. Carrier injection means optical modulation is possible	
xii. Thermo-optic effect means a second possibility for optical modulation exists	

Isotropic, Anisotropic and Dry Etching

- Typical isotropic etchants are mixtures of hydrofluoric, nitric and acetic acids.
- Typical anisotropic etchants are hot alkaline solutions such as aqueous potassium hydroxide (KOH), aqueous sodium hydroxide (NaOH), and EDP (a mixture of ethylenediamine, pyrocatechol and water)
- Dry etching techniques can be used, such as reactive ion etching, which also tend to be anisotropic etches as they are typically related to the angle at which the etching beam or plasma impinges on the silicon.

Figure 4.25 Silicon crystal structure.

Isotropic vs Anisotropic Etching

- In general, the {111} planes tend to etch slowly, the {110} planes rapidly, and the {100} planes at an intermediate rate

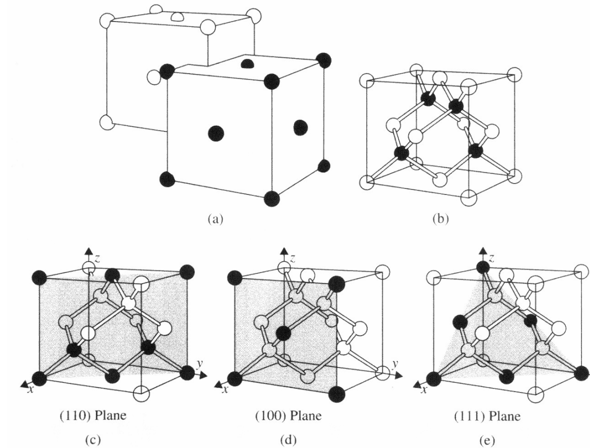

Figure 4.25 Silicon crystal structure.

Anisotropic Etching

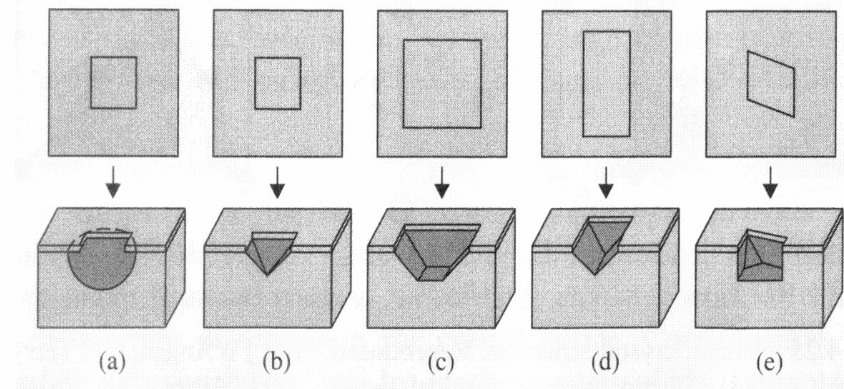

Figure 4.26 Etching of silicon via isotropic and anisotropic etches.

Example

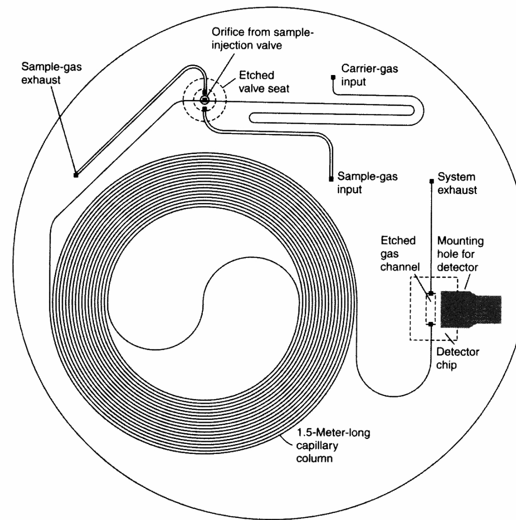

Figure 4.27 Example schematic of a complex shape etched into a silicon wafer.

Etched V-groove

- Etched V-groove, into which optical fibers are fixed in order to achieve good alignment with optical waveguides.

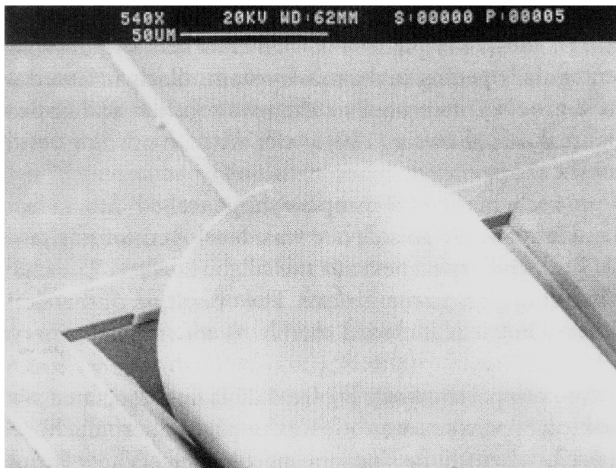

Figure 4.28 Optical fiber in a V-groove.